Note : This problem is taken from the book "Computational Fluid Dynamics the Basics with Applications" by JD Anderson (Page 285-325)

"

Numerical Solutions of Quasi-One-Dimensional Nozzle Flows

1. CFD Solution of Subsonic-Supersonic Isentropic Nozzle Flow: MacCormack's Technique

1.1 The Setup

We will set up three eschelons of equations as follows:

1. The governing flow equations will be couched in terms of partial differential equations suitable for the time-marching solution of quasi-one-dimensional flow.
2. The finite-difference expressions pertaining to MacCormack's technique as applied to this problem will be set up.
3. Other details for the numerical solution (such as the calculation of the time step and the treatment of boundary conditions) will be formulated.

The Governing Flow Equations:

In reality, the real nozzle flow is a two-dimensional flow because, with the area changing as a function of x, in actuality there will be flow-field variations in both the x and y directions. The assumption of quasi-one-dimensional flow dictates that the flow properties are functions of x only. The equations that are appropriate for quasi-one-dimensional flow, we would at least like for the overall physical principles of (1) mass conservation, (2) Newton's second law, and (3) energy conservation to hold exactly. To ensure that these physical principles are satisfied , we must use integral forms of the governing equations and apply these integral forms to a control volume consistent with the quasi-one-dimensional assumption. Let us proceed.

We start with the integral form of the continuity equation given by

$$\frac{\partial}{\partial t}\iiint_V \rho dV + \iint_S \rho \overrightarrow{V}.\overrightarrow{dS} = 0 \qquad (1)$$

We apply this equation to the shaded control volume in the Fig. 1. This control volume is a slice of the nozzle flow, where the infinitesimal thickness of the slice is dx. On the left side of the control volume, consistent with the quasi-one-dimensional assumption, the density, velocity, pressure, and internal energy, denoted by ρ , V , p and e, respectively, are uniform over the area A. Similarly, on the right side of the control volume, the density, velocity, pressure, and internal energy, denoted by $\rho + d\rho$, $V + dV$,

$p+dp$, and $e+de$, respectively , are uniform over the area $A+dA$. Applied to the control volume in Fig. 7.3, the volume integral in Eq. (2.16) becomes, in the limit as dx becomes very small,

$$\frac{\partial}{\partial t}\iiint_V \rho dV = \frac{\partial}{\partial t}(\rho A dx) \tag{2}$$

Where Adx is the volume of the control volume in the limit of dx becoming vanishingly small. The surface integral in Eq. (1) becomes

$$\iint_S \rho \vec{V}.\,\vec{dS} = -\rho VA + (\rho + d\rho)(V + dV)(A + dA) \tag{3}$$

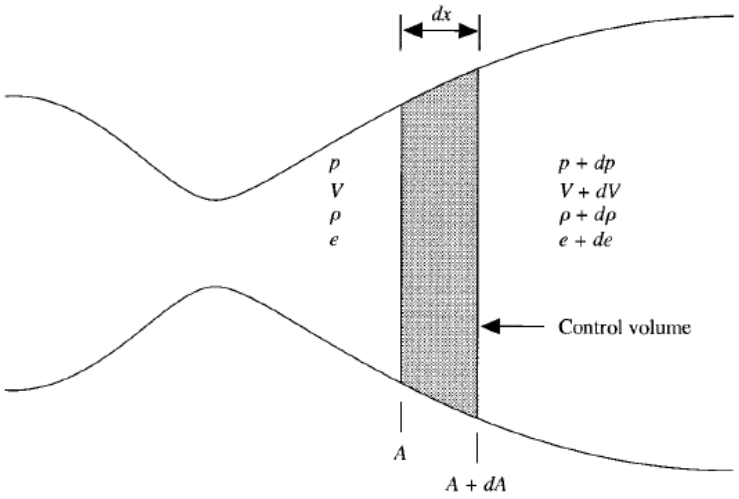

Fig.1. Control Volume for deriving the partial differential equations for unsteady,quasi-one-dimensional flow.

where the minus sign on the leading term on the right-hand side is due to the vectors $\vec{V}$ and $\vec{dS}$ pointing in opposition directions over the left face of the control volume, and hence the dot product is negative. Expanding the triple product term in Eq. (3) , we have

$$\iint_S \rho \vec{V}.\,\vec{dS} = -\rho VA + \rho VA + \rho V dA + \rho A dV + \rho dV dA + AV d\rho + V dA d\rho + A dV d\rho + d\rho dV dA \tag{4}$$

In the limit as dx becomes very small, the terms involving products of differentials in Eq. (4), such as $\rho dV dA$, $d\rho dV dA$, go to zero much faster than those terms involving products of differentials can be dropped, yielding in the limit as dx becomes very small

$$\iint_S \rho \vec{V}.\,\vec{dS} = \rho V dA + \rho A dV + AV d\rho = d(\rho AV) \tag{5}$$

Substituting Eqs. (2) and (5) into (1), we have

$$\frac{\partial}{\partial t}(\rho A dx) + d(\rho AV) = 0 \tag{6}$$

Dividing Eq. (6) by dx and noting that $d(\rho AV)/dx$ is, in the limit as dx goes to zero, the definition of the partial derivative with respect to x, we have

$$\frac{\partial(\rho A)}{\partial t}+\frac{\partial(\rho AV)}{\partial x}=0 \tag{7}$$

Equation (7) is the partial differential equation form of the continuity equation suitable for unsteady, quasi-one-dimensional flow. It ensures that mass is conserved for this model of the flow.

It is interesting to pause for a moment and compare this with the general continuity equation for 3D flow, specialized for 1D. For such a case,

$$\frac{\partial \rho}{\partial t}+\frac{\partial(\rho u)}{\partial x}=0 \tag{8}$$

where u is the x component of velocity. Clearly, Eq. (8) is different from Eq. (7) applies to a truly one-dimensional flow, where A is constant with respect to x. It doesn't represent a proper statement of the conservation of mass for our model of quasi-one-dimensional flow, where A = A(x); instead, Eq. (7) is a proper statement of mass conservation for our model. Of course, note that for the special case of constant-area flow, Eq. (7) reduces to Eq. (8).

We now turn to the integral form of the x component of the momentum equation, written below for an inviscid flow (neglecting viscous stress terms) with no body forces,

$$\frac{\partial}{\partial t}\iiint_V(\rho u)\,dV+\iint_S\left(\rho u\vec{V}\right).\vec{dS}=-\iint_S(pdS)_x \tag{9}$$

where the term $(pdS)_x$ denotes the x component of the vector $p\vec{dS}$. We apply Eq. (9) to the shaded control volume in Fig. 1. In Eq. (9) , the integrals on the left side are evaluated in the same manner as discussed above in regard to the continuity equation. That is,

$$\frac{\partial}{\partial t}\iiint_V(\rho u)\,dV=\frac{\partial}{\partial t}(\rho V A dx) \tag{10}$$

and

$$\iint_S\left(\rho u\vec{V}\right).\vec{dS}=-\rho V^2A+(\rho+d\rho)(V+dV)^2(A+dA) \tag{11}$$

The evaluation of the pressure force term on the right-hand side of Eq. (9) is best carried out with the aid of Fig. 2. Here, the x components of the vector $p\vec{dS}$ are shown on all four sides of the control volume. Remember that $\vec{dS}$ always points away from the control volume; hence any x component $(pdS)_x$ that acts toward the right (in the positive x direction) is a positive quantity. Also note that the x component of $p\vec{dS}$ acting on the top and bottom inclined faces of the control volume in Fig. 2 can be expressed as the pressure p acting on the component of the inclined area projected perpendicular to the x direction, (dA)/2;

hence, the contribution of each inclined face (top or bottom) to the pressure integral in Eq. (9) is –p(dA/2). All together, the right-hand side of Eq. (9) is expressed as follows :

$$\iint_S (pdS)_x = -pA + (p+dp)(A+dA) - 2p\left(\frac{dA}{2}\right) \tag{12}$$

Substituting Eqs. (10) to (12) into (9), we have

$$\frac{\partial}{\partial t}(\rho V A dx) + d(\rho V^2 A) = -A dp \tag{13}$$

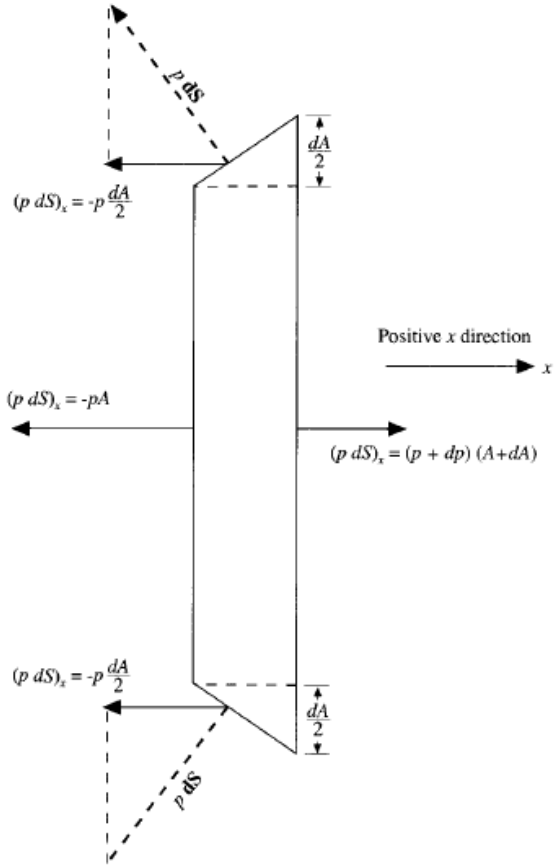

Fig.2. The forces in the x direction acting on the control volume

Dividing Eq. (13) by dx and taking the limit as dx goes to zero, we obtain the partial differential equation

$$\frac{\partial(\rho VA)}{\partial t} + \frac{\partial(\rho V^2 A)}{\partial x} = -A\frac{\partial p}{\partial x} \tag{14}$$

We could live with Eq. (14) as it stands-it represents the conservation form of the momentum equation for quasi-one-dimensional flow. However, let us obtain the equivalent nonconservation form. This is done by multiplying the continuity equation, Eq. (7) by V, obtaining

$$V\frac{\partial(\rho A)}{\partial t}+V\frac{\partial(\rho VA)}{\partial x}=0 \tag{15}$$

and then subtracting Eq. (15) from Eq. (14)

$$\frac{\partial(\rho VA)}{\partial t}-V\frac{\partial(\rho A)}{\partial t}+\frac{\partial\left(\rho V^2A\right)}{\partial x}-V\frac{\partial(\rho VA)}{\partial x}=-A\frac{\partial p}{\partial x} \tag{16}$$

Expanding the derivatives on the left-hand side of Eq. (16) and canceling like terms, we have

$$\rho A\frac{\partial V}{\partial t}+\rho AV\frac{\partial V}{\partial x}=-A\frac{\partial p}{\partial x} \tag{17}$$

Dividing Eq. (17) by A, we finally obtain

$$\rho\frac{\partial V}{\partial t}+\rho V\frac{\partial V}{\partial x}=-\frac{\partial p}{\partial x} \tag{18}$$

Eq. (18) is the momentum equation appropriate for quasi-one-dimensional flow, written in nonconservative form.

One of the reasons for obtaining the nonconservation form of the momentum equation is to compare it with the general result expressed by the following equation. For one-dimensional flow with no body forces, the following equation is written as

$$\rho\frac{\partial u}{\partial t}+\rho u\frac{\partial u}{\partial x}=-\frac{\partial p}{\partial x} \tag{19}$$

This is stylistically the same form as Eq. (18) for quasi-one-dimensional flow. Equations (18) and (19) simply demonstrate that the classic form of Euler's equation, generally written as

$$dp=-\rho VdV$$

holds for both types of flow.

Finally, let us consider the integral form of the energy equation. For an adiabatic flow ($\dot{q}=0$) with no body forces and no viscous effects, the integral form of the energy equation is

$$\frac{\partial}{\partial t}\iiint_V\rho\left(e+\frac{V^2}{2}\right)dV+\iint_S\rho\left(e+\frac{V^2}{2}\right)\vec{V}.\vec{dS}=-\iint_S\left(p\vec{V}\right).\vec{dS} \tag{20}$$

Applied to the shaded control volume in Fig.1. , and keeping in mind the pressure forces shown in Fig.2, Eq. (20) becomes

$$\frac{\partial}{\partial t}\left[\rho\left(e+\frac{V^2}{2}\right)Adx\right]-\rho\left(e+\frac{V^2}{2}\right)VA+\left(\rho+d\rho\right)\left[e+de+\frac{\left(V+dV\right)^2}{2}\right]\left(V+dV\right)\left(A+dA\right)$$

$$= -\left[-pVA + (p + dp)(V + dV)(A + dA) - 2\left(pV\frac{dA}{2} \right) \right] \tag{21}$$

Neglecting products of differentials and canceling like terms, Eq. (21) becomes

$$\frac{\partial}{\partial t}\left[\rho\left(e + \frac{V^2}{2} \right) A dx \right] + d(\rho eVA) + \frac{d(\rho V^3 A)}{2} = -d(pAV) \tag{22}$$

Or

$$\frac{\partial}{\partial t}\left[\rho\left(e + \frac{V^2}{2} \right) A dx \right] + d\left[\rho\left(e + \frac{V^2}{2} \right) VA \right] = -d(pAV) \tag{23}$$

Taking the limit as dx approaches zero, Eq. (23), becomes the following partial differential equation:

$$\frac{\partial\left[\rho\left(e + V^2/2 \right) A \right]}{\partial t} + \frac{\partial\left[\rho\left(e + V^2/2 \right) VA \right]}{\partial x} = -\frac{\partial(pAV)}{\partial x} \tag{24}$$

Equation (24) is the conservation form of the energy equation expressed in terms of the total energy $e + V^2/2$, appropriate for unsteady, quasi-one-dimensional flow. Let us obtain from Eq. (24) the nonconservation form expressed in terms of internal energy by itself. The latter can be achieved by multiplying Eq. (14) by V, obtaining

$$\frac{\partial\left[\rho\left(V^2/2 \right) A \right]}{\partial t} + \frac{\partial\left[\rho\left(V^3/2 \right) A \right]}{\partial x} = -AV\frac{\partial p}{\partial x} \tag{25}$$

and subtracting Eq. (25) from (24), yielding

$$\frac{\partial(\rho eA)}{\partial t} + \frac{\partial(\rho eVA)}{\partial x} = -p\frac{\partial(AV)}{\partial x} \tag{26}$$

Equation (26) is the conservation form of the energy equation expressed in terms of internal energy e, suitable for quasi-one-dimensional flow. The nonconservation form is then obtained by multiplying the continuity equation, Eq. 7, by e ,

$$e\frac{\partial(\rho A)}{\partial t} + e\frac{\partial(\rho AV)}{\partial x} = 0 \tag{27}$$

and subtracting Eq. (27) from Eq. (26), yielding

$$\rho A\frac{\partial e}{\partial t} + \rho AV\frac{\partial e}{\partial x} = -p\frac{\partial(AV)}{\partial x} \tag{28}$$

Expanding the right-hand side and dividing by A , Eq. (28) becomes

$$\rho\frac{\partial e}{\partial t}+\rho V\frac{\partial e}{\partial x}=-p\frac{\partial V}{\partial x}-p\frac{V}{A}\frac{\partial A}{\partial x} \tag{29}$$

or ,

$$\rho\frac{\partial e}{\partial t}+\rho V\frac{\partial e}{\partial x}=-p\frac{\partial V}{\partial x}-pV\frac{\partial(\ln A)}{\partial x} \tag{30}$$

Equation (30) is the nonconservation form of the energy equation expressed in terms of internal energy, appropriate to unsteady, quasi-one-dimensional flow.

The reason for obtaining the energy equation in the form of Eq. (30) is that, for a calorically perfect gas, it leads directly to a form of the energy equation in terms of temperature T. For our solution of the quasi-one-dimensional nozzle flow of a calorically perfect gas, this is a fundamental variable, and therefore it is convenient to deal with it as the primary dependent variable in the energy equation. For a calorically perfect gas

$$e=c_v T$$

Hence, Eq. (30) becomes

$$\rho c_v\frac{\partial T}{\partial t}+\rho V c_v\frac{\partial T}{\partial x}=-p\frac{\partial V}{\partial x}-pV\frac{\partial(\ln A)}{\partial x} \tag{31}$$

As an interim summary, our continuity, momentum and energy equations for unsteady, quasi-one-dimensional flow are given by Eqs. (7), (18) and (31), respectively. Take the time to look at these equations; you see three equations with four unknown variables ρ , V, p and T. The pressure can be eliminated from these equations by using the equation of state

$$p=\rho RT \tag{32}$$

along with its derivative

$$\frac{\partial p}{\partial x}=R\left(\rho\frac{\partial T}{\partial x}+T\frac{\partial\rho}{\partial x}\right) \tag{33}$$

With this, we expand Eq. (7) and rewrite Eqs. (18) and (31), respectively, as

Continuity: $$\frac{\partial(\rho A)}{\partial t}+\rho A\frac{\partial V}{\partial x}+\rho V\frac{\partial A}{\partial x}+VA\frac{\partial\rho}{\partial x}=0 \tag{34}$$

Momentum: $$\rho\frac{\partial V}{\partial t}+\rho V\frac{\partial V}{\partial x}=-R\left(\rho\frac{\partial T}{\partial x}+T\frac{\partial\rho}{\partial x}\right) \tag{35}$$

Energy: $$\rho c_v\frac{\partial T}{\partial t}+\rho V c_v\frac{\partial T}{\partial x}=-\rho RT\left(\frac{\partial V}{\partial x}+V\frac{\partial(\ln A)}{\partial x}\right) \tag{36}$$

At this stage, we could readily proceed to set up our numerical solution of Eqs. (34) to (36) . Note that these are written in terms of dimensional variables. This is fine, and many CFD solutions are carried out directly in terms of such dimensional variables. Indeed, this has an added engineering advantage because

it gives you a feeling for the magnitudes of the real physical quantities as the solution progresses. However, for nozzle flows, the flow-field variables are frequently expressed in terms of nondimensional variables. The nondimensional variables p/p_0, ρ/ρ_0 and T/T_0 vary between 0 and 1, which is an "aesthetic" advantage when presenting the results where p_0 , ρ_0 and T_0 are reservoir pressure, density and temperature respectively. We define the nondimensional temperature and density , respectively as

$$T' = \frac{T}{T_0} \qquad \rho' = \frac{\rho}{\rho_0}$$

where the prime denotes a dimensionless variable. Moreover, letting L denote the length of the nozzle, we define a dimensionless length as

$$x' = \frac{x}{L}$$

Denoting the speed of sound in the reservoir as a_0, where

$$a_0 = \sqrt{\gamma R T_0}$$

We define a dimensionless velocity as

$$V' = \frac{V}{a_0}$$

Also, the quantity L/a_0 has the dimension of time, and we define a dimensionless time as

$$t' = \frac{t}{L/a_0}$$

Finally, we ratio the local area A to the sonic throat area A^* and define a dimensionless area as

$$A' = \frac{A}{A^*}$$

Returning to Eq. (34) and introducing the nondimensional variables, we have

$$\frac{\partial(\rho'A')}{\partial t'}\left(\frac{\rho_0 A^*}{L/a_0}\right) + \rho'A'\frac{\partial V'}{\partial x'}\left(\frac{\rho_0 A^* a_0}{L}\right) + \rho'V'\frac{\partial A'}{\partial x'}\left(\frac{\rho_0 a_0 A^*}{L}\right) + V'A'\frac{\partial \rho'}{\partial x'}\left(\frac{a_0 A^* \rho_0}{L}\right) = 0 \qquad (37)$$

Note that A' is a function of x' only ; it is not a function of time (the nozzle geometry is fixed, invariant with time). Hence, in Eq. (37) the time derivative can be written as

$$\frac{\partial(\rho'A')}{\partial t'} = A'\frac{\partial \rho'}{\partial t'}$$

With this, Eq. (37) becomes

Continuity :
$$\frac{\partial \rho'}{\partial t'} = -\rho' \frac{\partial V'}{\partial x'} - \rho' V' \frac{\partial (\ln A')}{\partial x'} - V' \frac{\partial \rho'}{\partial x'} \tag{38}$$

Returning to Eq. (35) and introducing the nondimensional variables, we have

$$\rho' \frac{\partial V'}{\partial t'} \left(\frac{\rho_0 a_0}{L / a_0} \right) + \rho' V' \frac{\partial V'}{\partial x'} \left(\frac{\rho_0 a_0^2}{L} \right) = -R \left(\rho' \frac{\partial T'}{\partial x'} + T' \frac{\partial \rho'}{\partial x'} \right) \left(\frac{\rho_0 T_0}{L} \right)$$

or
$$\rho' \frac{\partial V'}{\partial t'} = -\rho' V' \frac{\partial V'}{\partial x'} - \left(\rho' \frac{\partial T'}{\partial x'} + T' \frac{\partial \rho'}{\partial x'} \right) \frac{R T_0}{a_0^2} \tag{39}$$

In Eq. (39) , note that

$$\frac{R T_0}{a_0^2} = \frac{\gamma R T_0}{\gamma a_0^2} = \frac{a_0^2}{\gamma a_0^2} = \frac{1}{\gamma}$$

Momentum :
$$\frac{\partial V'}{\partial t'} = -V' \frac{\partial V'}{\partial x'} - \frac{1}{\gamma} \left(\frac{\partial T'}{\partial x'} + \frac{T'}{\rho'} \frac{\partial \rho'}{\partial x'} \right) \tag{40}$$

Returning to Eq. (36) and introducing the nondimensional variables, we have

$$\rho' c_v \frac{\partial T'}{\partial t'} \left(\frac{\rho_0 T_0}{L / a_0} \right) + \rho' V' c_v \frac{\partial T'}{\partial x'} \left(\frac{\rho_0 a_0 T_0}{L} \right) = -\rho' R T' \left(\frac{\partial V'}{\partial x'} + V' \frac{\partial (\ln A')}{\partial x'} \right) \left(\frac{\rho_0 T_0 a_0}{L} \right) \tag{41}$$

In Eq. (41), the factor R / c_v is given by

$$\frac{R}{c_v} = \frac{R}{R / (\gamma - 1)} = \gamma - 1$$

Hence, Eq. (41) becomes

Energy :
$$\frac{\partial T'}{\partial t'} = -V' \frac{\partial T'}{\partial x'} - (\gamma - 1) T' \left(\frac{\partial V'}{\partial x'} + V' \frac{\partial (\ln A')}{\partial x'} \right) \tag{42}$$

THE FINITE-DIFFERENCE EQUATIONS:

We now proceed to the next eschelon, namely, the setting up of the finite-difference expressions using MacCormack's explicit technique for the numerical solution of Eqs. (38) , (40) and (42). To implement a finite-difference solution, we divide the x axis along the nozzle into a number of discrete grid points, as shown in Fig. 3. (Recall that in our quasi-one-dimensional nozzle assumption, the flow variables across the nozzle cross section at any particular grid point, say point i, are uniform). In Fig. 3, the first grid point, labeled point 1, is assumed to be in the reservoir. The points are evenly distributed along the x axis, with Δx denoting the spacing between grid points. The last point, namely, that at the nozzle exit, is denoted by

N; we have a total number of N grid points distributed along the axis. Point i is simply an arbitrary grid point, with points i-1 and i+1 as the adjacent points. In the time-marching approach, remember that we know the flow-field variables at time t, and we use the difference equations to solve explicitly for the variables at time t+Δt.

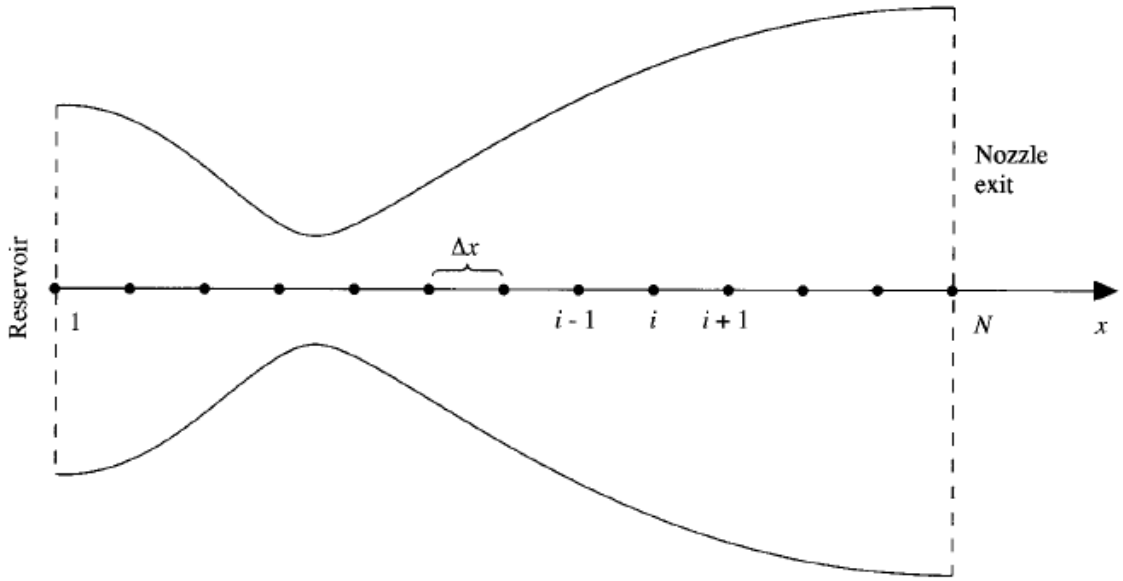

Fig. 3. Grid point distribution along the nozzle

MacCormack's Explicit Technique

MacCormack's technique is a variant of the Lax-Wendroff approach but is much simpler in its application. Like the Lax-Wendroff method, the MacCormack method is also an explicit finite-difference technique which is second order accurate in both space and time.

Consider the two dimensional grid shown in fig. below.

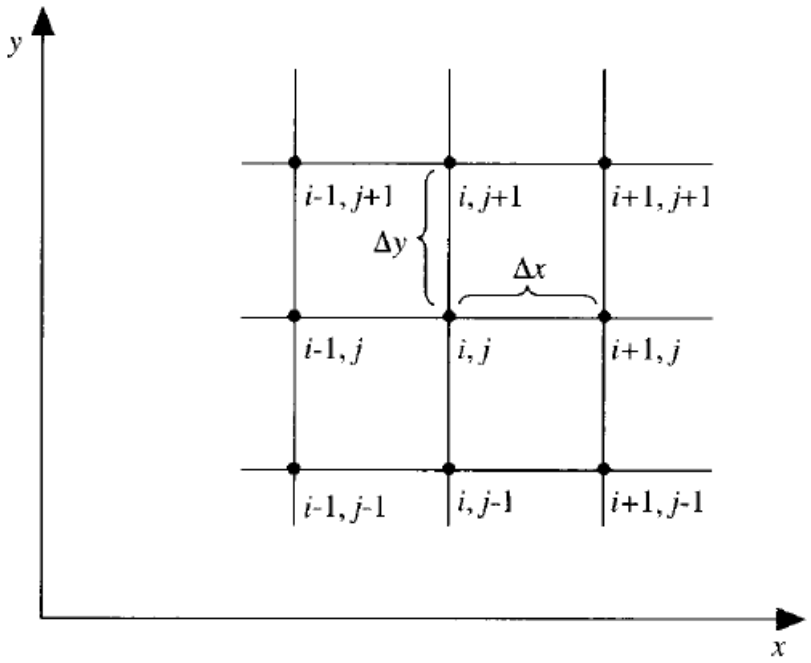

Fig. 1 Rectangular grid segment

For purposes of illustration, let us address the solution of the Euler equations given below.

Continuity : $$\frac{\partial \rho}{\partial t} = -\left(\rho \frac{\partial u}{\partial x} + u \frac{\partial \rho}{\partial x} + \rho \frac{\partial v}{\partial y} + v \frac{\partial \rho}{\partial y} \right) \quad \text{(A)}$$

x momentum : $$\frac{\partial u}{\partial t} = -\left(u \frac{\partial u}{\partial x} + v \frac{\partial u}{\partial x} + \frac{1}{\rho} \frac{\partial p}{\partial y} \right) \quad \text{(B)}$$

y momentum : $$\frac{\partial v}{\partial t} = -\left(u \frac{\partial v}{\partial x} + v \frac{\partial v}{\partial y} + \frac{1}{\rho} \frac{\partial p}{\partial y} \right) \quad \text{(C)}$$

Energy : $$\frac{\partial e}{\partial t} = -\left(u \frac{\partial e}{\partial x} + v \frac{\partial e}{\partial y} + \frac{p}{\rho} \frac{\partial u}{\partial x} + \frac{p}{\rho} \frac{\partial v}{\partial y} \right) \quad \text{(D)}$$

In the above equations, we have assumed no body forces and no volumetric heat addition; that is, $\vec{f} = 0$ and $\dot{q} = 0$ .Equation (A) to (D) are hyperbolic with respect to time.

Here, we address time-marching solution using MacCormack's technique. As before, we assume that the flow field at each grid point is known at time t, and we proceed to calculate the flow-field variables at the same grid points at time $t + \Delta t$, as in figure below.

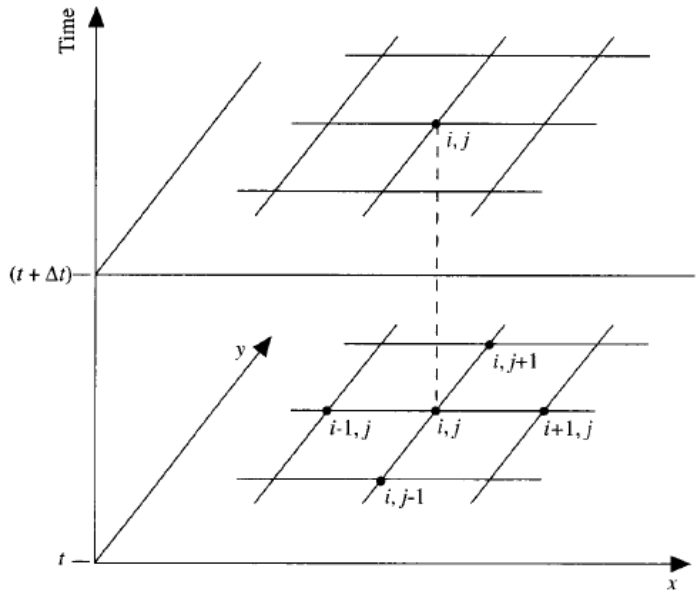

Fig. 2 A schematic of the grid for time marching

First, consider the density at grid point (i,j) at time $t+\Delta t$. In MacCormack's method, this is obtained from

$$\rho_{i,j}^{t+\Delta t} = \rho_{i,j}^{t} + \left(\frac{\partial \rho}{\partial t}\right)_{av} \Delta t \qquad \text{(I)}$$

where $\left(\frac{\partial \rho}{\partial t}\right)_{av}$ is a representative mean value of $\frac{\partial \rho}{\partial t}$ between times t and $t+\Delta t$.

Similar relations are written for the other flow-field variables.

$$u_{i,j}^{t+\Delta t} = u_{i,j}^{t} + \left(\frac{\partial u}{\partial t}\right)_{av} \Delta t \qquad \text{(II)}$$

$$v_{i,j}^{t+\Delta t} = v_{i,j}^{t} + \left(\frac{\partial v}{\partial t}\right)_{av} \Delta t \qquad \text{(III)}$$

$$e_{i,j}^{t+\Delta t} = e_{i,j}^{t} + \left(\frac{\partial e}{\partial t}\right)_{av} \Delta t \qquad \text{(IV)}$$

Let us illustrate by using the calculation of density as an example. Return to Eq.(I). The average time derivative, $\left(\frac{\partial \rho}{\partial t}\right)_{av}$, is obtained from a predictor-corrector philosophy as follows :

Predictor Step : In the continuity equation,Eq. (A),replace the spatial derivatives on the RHS with forward differences.

$$\left(\frac{\partial \rho}{\partial t}\right)_{i,j}^{t} = -\left(\rho_{i,j}^{t}\frac{u_{i+1,j}^{t}-u_{i,j}^{t}}{\Delta x}+u_{i,j}^{t}\frac{\rho_{i+1,j}^{t}-\rho_{i,j}^{t}}{\Delta x}+\rho_{i,j}^{t}\frac{v_{i,j+1}^{t}-v_{i,j}^{t}}{\Delta y}+v_{i,j}^{t}\frac{\rho_{i+1,j}^{t}-\rho_{i,j}^{t}}{\Delta y}\right) \quad \text{(V)}$$

In Eq. (V) , all flow variables at time t are known values; i.e., the right-hand side is known. Now, obtain a predicted value of density, $\left(\overline{\rho}\right)^{t+\Delta t}$, from the first two terms of a Taylor series, as follows.

$$\left(\overline{\rho}\right)_{i,j}^{t+\Delta t} = \rho_{i,j}^{t} + \left(\frac{\partial \rho}{\partial t}\right)_{i,j}^{t}\Delta t \quad \text{(VI)}$$

In Eq. (VI) , $\rho_{i,j}^{t}$ is known, and $\left(\frac{\partial \rho}{\partial t}\right)_{i,j}^{t}$ is a known number from Eq. (V) ; hence $\left(\overline{\rho}\right)_{i,j}^{t+\Delta t}$ is readily obtained.

The value of $\left(\overline{\rho}\right)_{i,j}^{t+\Delta t}$ is only a predicted value of density; it is only first-order-accurate since Eq. (VI) contains only the first-order terms in the Taylor series.

In a similar fashion, predicted values for u, v and e can be obtained, i.e.,

$$\left(\overline{u}\right)_{i,j}^{t+\Delta t} = u_{i,j}^{t} + \left(\frac{\partial u}{\partial t}\right)_{i,j}^{t}\Delta t \quad \text{(VII)}$$

$$\left(\overline{v}\right)_{i,j}^{t+\Delta t} = v_{i,j}^{t} + \left(\frac{\partial v}{\partial t}\right)_{i,j}^{t}\Delta t \quad \text{(VIII)}$$

$$\left(\overline{e}\right)_{i,j}^{t+\Delta t} = e_{i,j}^{t} + \left(\frac{\partial e}{\partial t}\right)_{i,j}^{t}\Delta t \quad \text{(IX)}$$

In Eq (VII) to (IX) , numbers from the time derivatives on the right-hand side are obtained from Eqs. (B) to (D), respectively, with forward differences used for spatial derivatives, similar to those shown in Eq. (V) for the continuity equation.

Corrector Step: In the corrector step, we first obtain a predicted value of the time derivative at time $t+\Delta t$, $\left(\overline{\frac{\partial \rho}{\partial t}}\right)_{i,j}^{t+\Delta t}$, by substituting the predicted values of ρ, u, and v into the right side of the continuity equation, replacing the spatial derivatives with rearward differences.

$$\left(\overline{\frac{\partial \rho}{\partial t}}\right)_{i,j}^{t+\Delta t} = -\left[\left(\overline{\rho}\right)_{i,j}^{t+\Delta t}\frac{\left(\overline{u}\right)_{i,j}^{t+\Delta t}-\left(\overline{u}\right)_{i-1,j}^{t+\Delta t}}{\Delta x}+\left(\overline{u}\right)_{i,j}^{t+\Delta t}\frac{\left(\overline{\rho}\right)_{i,j}^{t+\Delta t}-\left(\overline{\rho}\right)_{i-1,j}^{t+\Delta t}}{\Delta x}+\left(\overline{\rho}\right)_{i,j}^{t+\Delta t}\frac{\left(\overline{v}\right)_{i,j}^{t+\Delta t}-\left(\overline{v}\right)_{i,j-1}^{t+\Delta t}}{\Delta y}\right.$$

$$\left.+\left(\overline{v}\right)_{i,j}^{t+\Delta t}\frac{\left(\overline{\rho}\right)_{i,j}^{t+\Delta t}-\left(\overline{\rho}\right)_{i,j-1}^{t+\Delta t}}{\Delta y}\right] \quad \text{(X)}$$

The average value of the time derivative of density which appears in Eq. (I) is obtained from the arithmetic mean of $\left(\frac{\partial \rho}{\partial t}\right)_{i,j}^{t}$, obtained from Eq. (V) and $\left(\overline{\frac{\partial \rho}{\partial t}}\right)_{i,j}^{t+\Delta t}$, obtained from Eq. (X).

$$\left(\frac{\partial \rho}{\partial t}\right)_{av} = \frac{1}{2}\left[\underbrace{\left(\frac{\partial \rho}{\partial t}\right)_{i,j}^{t}}_{\text{From Eq. (V)}} + \underbrace{\left(\overline{\frac{\partial \rho}{\partial t}}\right)_{i,j}^{t+\Delta t}}_{\text{From Eq. (X)}}\right] \tag{XI}$$

This allows us to obtain the final, "corrected" value of density at time $t + \Delta t$ from Eq. (I), repeated below:

$$\rho_{i,j}^{t+\Delta t} = \rho_{i,j}^{t} + \left(\frac{\partial \rho}{\partial t}\right)_{av} \Delta t \tag{I}$$

The predictor-corrector sequence described above yields the value of density at grid point (i,j) at time $t + \Delta t$ as illustrated in Fig. 2. This sequence is repeated at all grid points to obtain the density throughout the flow field at time $t + \Delta t$. To calculate u,v and e at time $t + \Delta t$, the same technique is used, starting with Eqs. (II) to (IV) and utilizing the momentum and energy equations in the form of Eqs. (B) to (D) to obtain the average time derivatives via the predictor-corrector sequence, using forward differences on the predictor and rearward differences on the corrector.

MacCormack's technique as described above, because a two-step predictor-corrector sequence is used with forward differences on the predictor and with rearward differences on the corrector, is a second-order-accurate method.

First, consider the predictor step. Following the discussion above, we set up the spatial derivatives as forward differences. Also, to reduce the complexity of the notation, we will drop the use of the prime to denote a dimensionless variable. In what follows, all variables are the nondimensional variables, denoted earlier by the prime notation. Analogous to Eq. (V), from Eq. (38) we have

$$\left(\frac{\partial \rho}{\partial t}\right)_{i,j}^{t} = -\rho_i^t \frac{V_{i+1}^t - V_i^t}{\Delta x} - \rho_i^t V_i^t \frac{\ln A_{i+1} - \ln A_i}{\Delta x} - V_i^t \frac{\rho_{i+1}^t - \rho_i^t}{\Delta x} \tag{43}$$

From Eq. (40), we have

$$\left(\frac{\partial V}{\partial t}\right)_{i}^{t} = -V_i^t \frac{V_{i+1}^t - V_i^t}{\Delta x} - \frac{1}{\gamma}\left(\frac{T_{i+1}^t - T_i^t}{\Delta x} + \frac{T_i^t}{\rho_i^t}\frac{\rho_{i+1}^t - \rho_i^t}{\Delta x}\right) \tag{44}$$

From Eq. (42) , we have

$$\left(\frac{\partial T}{\partial t}\right)_i^t = -V_i^t \frac{T_{i+1}^t - T_i^t}{\Delta x} - (\gamma - 1) T_i^t \left(\frac{V_{i+1}^t - V_i^t}{\Delta x} + V_i^t \frac{\ln A_{i+1} - \ln A_i}{\Delta x} \right)$$

(45)

```
    % Predictor Step
    for i = 2:k-1;
        V1 = (V(i+1)-V(i))/dx;
        lnA1 = (log(A(i+1))-log(A(i)))/dx;
        rho1 = (rho(i+1)-rho(i))/dx;
        T1 = (T(i+1)-T(i))/dx;
        drhodt_1(i) = -rho(i)*V1-rho(i)*V(i)*lnA1-
V(i)*rho1;                                          % eq. (43)
        dVdt_1(i) = -V(i)*V1-gamma1*T1-
gamma1*rho1*T(i)/rho(i);                          % eq. (44)
        dTdt_1(i) = -V(i)*T1-gamma2*T(i)*V1-
gamma2*T(i)*V(i)*lnA1;                            % eq. (45)
    end
```

Analogous to Eqs. (VI) to (X), we obtain predicted values of ρ, V, and T, denoted by barred quantities, from

$$\left(\bar{\rho}\right)_i^{t+\Delta t} = \rho_i^t + \left(\frac{\partial \rho}{\partial t}\right)_i^t \Delta t \tag{46}$$

$$\left(\bar{V}\right)_i^{t+\Delta t} = V_i^t + \left(\frac{\partial V}{\partial t}\right)_i^t \Delta t \tag{47}$$

$$\left(\bar{T}\right)_i^{t+\Delta t} T_i^t + \left(\frac{\partial T}{\partial t}\right)_i^t \Delta t \tag{48}$$

```
% predicted values
    for i = 2:k-1
        rho_p(i) = rho(i)+drhodt_1(i)*dt;   % eq. (46)
        V_p(i) = V(i)+dVdt_1(i)*dt;         % eq. (47)
        T_p(i) = T(i)+dTdt_1(i)*dt;         % eq. (48)
    end
```

In Eqs. (46) to (48), ρ_i^t, V_i^t, and T_i^t, are known values at time t. Numbers for the time derivatives in Eqs. (46) to (48) are supplied directly by Eqs. (43) to (45).

Moving to the corrector step, we return to Eqs. (38),(40) and (42) and replace the spatial derivatives with rearward differences, using the predicted (barred) quantities. Analogous to Eq. (XI), we have from Eq. (38).

$$\left(\frac{\overline{\partial\rho}}{\partial t}\right)_i^{t+\Delta t} = -\bar{\rho}_i^{t+\Delta t}\frac{\bar{V}_i^{t+\Delta t}-\bar{V}_{i-1}^{t+\Delta t}}{\Delta x} - \bar{\rho}_i^{t+\Delta t}\bar{V}_i^{t+\Delta t}\frac{\ln A_i - \ln A_{i-1}}{\Delta x} - \bar{V}_i^{t+\Delta t}\frac{\bar{\rho}_i^{t+\Delta t}-\bar{\rho}_{i-1}^{t+\Delta t}}{\Delta x} \tag{49}$$

From Eq. (40), we have

$$\left(\frac{\overline{\partial V}}{\partial t}\right)_i^{t+\Delta t} = -\bar{V}_i^{t+\Delta t}\frac{\bar{V}_i^{t+\Delta t}-\bar{V}_{i-1}^{t+\Delta t}}{\Delta x} - \frac{1}{\gamma}\left(\frac{\bar{T}_i^{t+\Delta t}-\bar{T}_{i-1}^{t+\Delta t}}{\Delta x} + \frac{\bar{T}_i^{t+\Delta t}}{\bar{\rho}_i^{t+\Delta t}}\frac{\bar{\rho}_i^{t+\Delta t}-\bar{\rho}_{i-1}^{t+\Delta t}}{\Delta x}\right) \tag{50}$$

From Eq. (42) , we have

$$\left(\frac{\overline{\partial T}}{\partial t}\right)_i^{t+\Delta t} = -\bar{V}_i^{t+\Delta t}\frac{\bar{T}_i^{t+\Delta t}-\bar{T}_{i-1}^{t+\Delta t}}{\Delta x} - (\gamma-1)\bar{T}_i^{t+\Delta t}\left(\frac{\bar{V}_i^{t+\Delta t}-\bar{V}_{i-1}^{t+\Delta t}}{\Delta x} + \bar{V}_i^{t+\Delta t}\frac{\ln A_i - \ln A_{i-1}}{\Delta x}\right) \tag{51}$$

```
% corrector step
    for i = 2:k-1;
        V1 = (V_p(i)-V_p(i-1))/dx;
        lnA1 = (log(A(i))-log(A(i-1)))/dx;
        rho1 = (rho_p(i)-rho_p(i-1))/dx;
        T1 = (T_p(i)-T_p(i-1))/dx;
        drhodt_2(i) = -rho_p(i)*V1-
rho_p(i)*V_p(i)*lnA1-V_p(i)*rho1;          % eq. (49)
        dVdt_2(i) = -V_p(i)*V1-gamma1*T1-
gamma1*rho1*T_p(i)/rho_p(i);          % eq. (50)
        dTdt_2(i) = -V_p(i)*T1-gamma2*T_p(i)*V1-
gamma2*T_p(i)*V_p(i)*lnA1;          % eq. (51)
    end
```

Analogous to Eq. (XI), the average time derivatives are given by

$$\left(\frac{\partial\rho}{\partial t}\right)_{av} = 0.5\left[\underbrace{\left(\frac{\partial\rho}{\partial t}\right)_i^t}_{\text{From Eq. (43)}} + \underbrace{\left(\frac{\overline{\partial\rho}}{\partial t}\right)_i^{t+\Delta t}}_{\text{From Eq. (49)}}\right] \tag{52}$$

$$\left(\frac{\partial V}{\partial t}\right)_{av} = 0.5\left[\underbrace{\left(\frac{\partial V}{\partial t}\right)_i^t}_{\text{From Eq. (44)}} + \underbrace{\left(\overline{\frac{\partial V}{\partial t}}\right)_i^{t+\Delta t}}_{\text{From Eq. (50)}}\right] \tag{53}$$

$$\left(\frac{\partial T}{\partial t}\right)_{av} = 0.5\left[\underbrace{\left(\frac{\partial T}{\partial t}\right)_i^t}_{\text{From Eq. (45)}} + \underbrace{\left(\overline{\frac{\partial T}{\partial t}}\right)_i^{t+\Delta t}}_{\text{From Eq. (51)}}\right] \tag{54}$$

```
% Average time derivatives

for i = 2:k-1;
 drhodt_av(i) = 0.5*(drhodt_1(i)+drhodt_2(i));% eq.(52)
 dVdt_av(i) = 0.5*(dVdt_1(i)+dVdt_2(i));      % eq.(53)
 dTdt_av(i) = 0.5*(dTdt_1(i)+dTdt_2(i));      % eq. (54)
end
```

Finally, analogous to Eqs. (I) to (IV), we have for the corrected values of the flow-field variables at time $t+\Delta t$

$$\rho_i^{t+\Delta t} = \rho_i^t + \left(\frac{\partial \rho}{\partial t}\right)_{av} \Delta t \tag{55}$$

$$V_i^{t+\Delta t} = V_i^t + \left(\frac{\partial V}{\partial t}\right)_{av} \Delta t \tag{56}$$

$$T_i^{t+\Delta t} = T_i^t + \left(\frac{\partial T}{\partial t}\right)_{av} \Delta t \tag{57}$$

Pseudocode:

```
% corrected values of flow field variables at time t+dt

    for i = 2:k-1
        rho(i) = rho(i)+drhodt_av(i)*dt;      % eq. (55)
        V(i) = V(i)+dVdt_av(i)*dt;            % eq. (56)
        T(i) = T(i)+dTdt_av(i)*dt;            % eq. (57)
        P(i) = rho(i)*T(i);
        M(i) = V(i)*T(i)^-0.5;
    end
```

Keep in mind that all variables in Eqs. (43) to (57) are the nondimensional values. Also, Eqs. (43) to (57) constitute our second orreder eschelon of equations, namely, the finite difference expressions of the governing equations in a form that pertains to MacCormack's technique.

CALCULATION OF TIME STEP:

We now proceed to third and final eschelon of equations mentioned at the beginning of this section, namely, the setting up other details necessary for the numerical solution of the quasi-one-dimensional to time and a nozzle flow problem. The governing equation is hyperbolic with respect time and so a stability constraint exists on this system, namely,

$$\Delta t = C\frac{\Delta x}{a + V} \tag{58}$$

where C is the Courant number, the simple stability analysis of a linear hyperbolic equation gives the result that $C \leq 1$ for an explicit numerical solution to be stable. The present application to subsonic-supersonic isentropic nozzle flow is governed by nonlinear partial differential equations. In this case , the exact stability criterion for a linear equation, namely, that $C \leq 1$, can only be viewed as general guidance for our present nonlinear problem. Equation (58) is the Courant-Friedrichs-Lowry (CFL) criterion for a one-dimensional flow, where V is the local flow velocity at a point in the flow and a is the local speed of sound. Equation (58) , along with $C \leq 1$, simply states that Δt must be less than , or at best equal to, the time it takes a sound wave to move from one grid point to the next. Equation (58) is in dimensional form. However, when t,x,a and V are nondimensionalized, the nondimensional form of Eq. (58) is exactly the same form as the dimensional case. Hence, we will hereafter treat the variables in Eq. (58) as our nondimensional variables defined earlier. That is, in Eq. (58), Δt is the increment in nondimensional time and Δx is the increment in nondimensional space; Δt and Δx in Eq. (58) are precisely the same as appear in the non-dimensional equations (43) to (57). Examining Eq.(58) more carefully, we note that, although Δx is same throughout the flow, both V and a are variables. Hence, at a given grid point at a given time step, Eq. (58) is written as

$$\left(\Delta t\right)_i^t = C\frac{\Delta x}{a_i^t + V_i^t} \tag{59}$$

At an adjacent grid point, we have from Eq. (58)

$$\left(\Delta t\right)_{i+1}^t = C\frac{\Delta x}{a_{i+1}^t + V_{i+1}^t} \tag{60}$$

For this problem, $a = \sqrt{T}$, so

$$\left(\Delta t\right)_i^t = C\frac{\Delta x}{\left(\sqrt{T}\right)_i^t + V_i^t}$$

Pseudocode:

```
for i = 1:k
      dta(i) = (c*dx)/(T(i)^0.5+V(i));
end
```

Clearly, $(\Delta t)_i^t$ and $(\Delta t)_{i+1}^t$ obtained from Eqs. (59) and (60), respectively are, in general, different values. Hence, in the implementation of the time-marching solution, we have two choices :

1. In utilizing Eqs. (46) to (48) and (55) to (57) ,we can, at each grid point i, employ the local values of $(\Delta t)_i^t$ determined from Eq. (59). In this fashion, the flow-field variables at each grid point in Fig.3 will be advanced in time according to their own, local time step. Hence, the resulting flow field at time $t + \Delta t$ will be in a type of artificial "time warp", with the flow-field variables at a given grid point corresponding to some nonphysical time different from that of the variables at an adjacent grid point. Clearly, such a local time-stepping approach does not realistically follow the actual, physical transients in the flow and hence cannot be used for an accurate solution of the unsteady flow. However, if the final steady-state flow field in the limit of large time is the only desired result, then the intermediate variation of the flow-field variables with time is irrelevant. Indeed, if such is the case, the local time stepping will frequently lead to faster convergence to the steady state. This is why some practitioners use the local time-stepping approach.

2. The other choice is to calculate $(\Delta t)_i^t$ at all grid points, i = 1 to i = N, and then choose the minimum value for use in Eqs. (46) to (48) and (55) to (57). That is,

$$\Delta t = \text{minimum}\left(\Delta t_1^t, \Delta t_2^t, ..., \Delta t_i^t, ..., \Delta t_N^t\right) \tag{61}$$

Pseudocode:

```
dt = min(dta);
```

The resulting Δt obtained from Eq. (61) is then used in Eqs. (46) to (48) and (55) to (57). In this fashion, the flow-field variables at all the grid points at time $t + \Delta t$ all correspond to the same physical time. Hence, the time-marching solution is following the actual unsteady flow variations that would exist in nature; i.e., the solution gives a time-accurate solution of the actual transient flow field, consistent with the unsteady continuity, momentum, and energy equations. This consistent time marching is the approach we will use. Although, it may require more time steps to approach the steady state in comparison to the "local" time stepping described earlier, we can feel comfortable that the consistent time-marching approach is giving us the physically meaningful transient variations-which frequently are intrinsic value by themselves. Thus, in our subsequent calculations, we will use Eq. (61) to determine the value of Δt .

BOUNDARY CONDITIONS:

Another aspect of the numerical solution is that of boundary conditions- an all important aspect, because without the physically implementation of boundary conditions and their numerically proper representation, we have no hope whatsoever in obtaining a proper numerically proper solution to our problem. First, let us examine the physical boundary conditions for the subsonic-supersonic isentropic flow. Returning to Fig. 3, we note that grid points 1 and N represent the two boundary points on the x axis. Point 1 is essentially in the reservoir; it represents an inflow boundary, with flow coming from the reservoir and entering the nozzle. In contrast, point N is an outflow boundary, with flow leaving the nozzle at the nozzle exit. Moreover, the flow velocity at point 1 is a very low, subsonic value. (The flow velocity at point 1, which corresponds to a finite area ratio A_1 / A^* ,cannot be precisely zero; if it were, there would be no mass flow entering the nozzle. Hence, point 1 does not correspond exactly to the reservoir, where by definition the flow velocity is zero. That is, the area for the reservoir is theoretically infinite, and we are clearly starting our own calculation at point 1 where the cross-sectional area is finite.) Hence, not only is point 1 an inflow boundary, it is a subsonic inflow boundary. We indicated that unsteady, inviscid flow is governed by hyperbolic equations, and therefore for one-dimensional unsteady flow there exist two real characteristics lines through any point in the xt plane. This is illustrated in Fig.4.

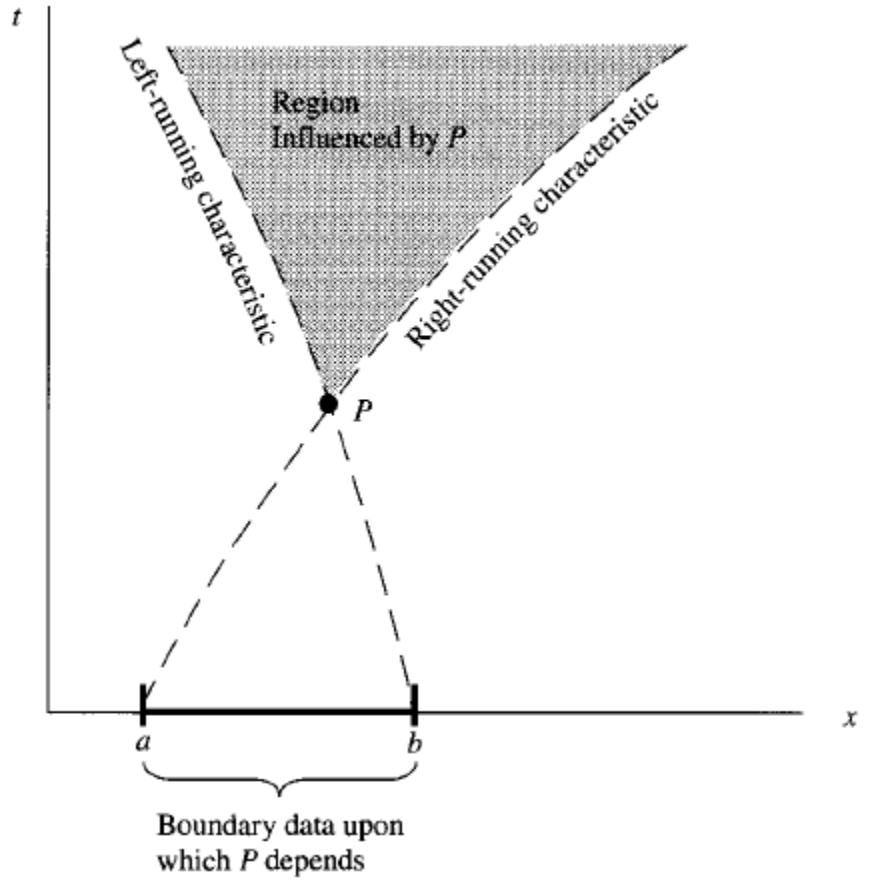

Fig. 4. Domain and boundaries for the solution of hyperbolic equations. One-dimensional unsteady flow

Note that the two characteristics lines through point P in Fig.4 are labeled left- and right-running characteristics respectively. Physically, these two characteristics represent infinitely weak Mach waves which are propagating upstream and downstream, respectively. Both waves are travelling at the speed of sound a. Now turn to Fig.5, which shows our convergent-divergent nozzle (Fig. 7.6a) with xt diagram sketched below it (Fig. 7.6b).

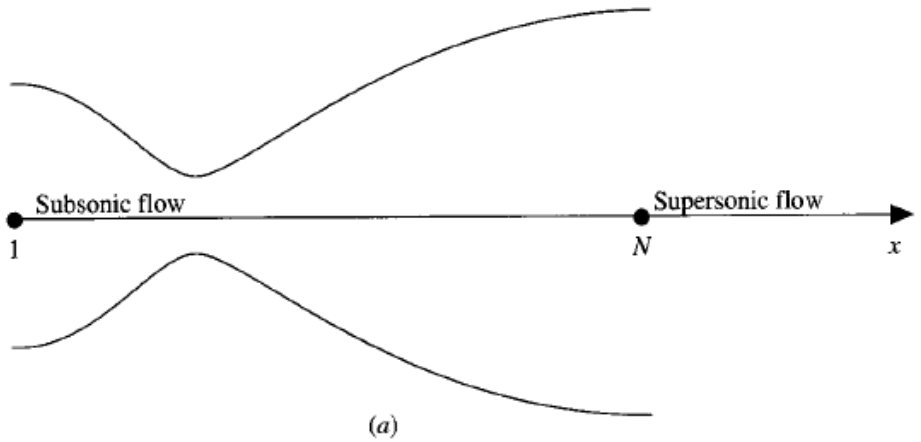

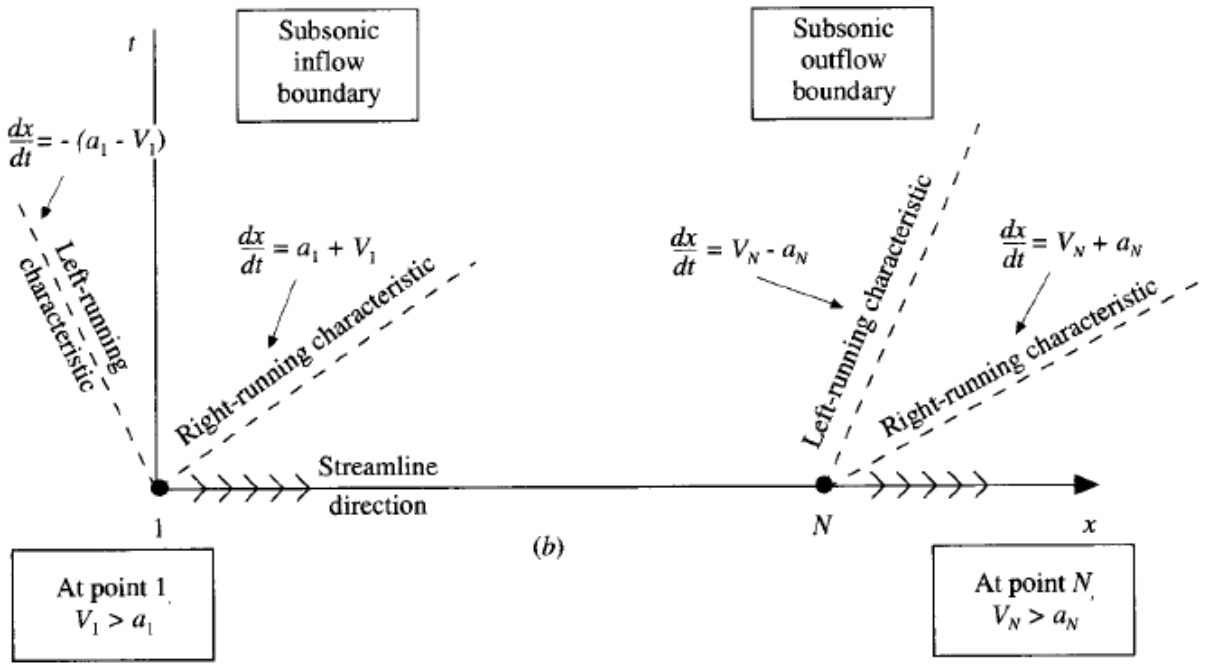

Fig.5. Study of boundary conditions: subsonic inflow and supersonic outflow

At point 1, the local flow velocity is subsonic, $V_1 < a_1$. Hence, the left-running characteristic at point 1 travels upstream, to the left in Fig. 5; i.e., the left-running Mach wave, which is travelling toward the left (relative to a moving fluid element) at the speed of sound easily works its way upstream against the low-velocity subsonic flow, which is slowly moving from left to right. Hence, in Fig. 5b, we show the left-running characteristic running to the left with a combined speed $a_1 - V_1$ (relative to the fixed nozzle in Fig.5). Since the domain for the fluid flow to be calculated is contained between grid points 1 and N, then at point 1 we see that the left-running characteristic is propagating out of the domain; it is propagating to the left, away from the domain. In contrast, the right-running characteristic, which is a Mach wave propagating toward the right in Fig. 5b. This is for two reasons: (1) the fluid element at point 1 is already moving toward the right, and (2) the right-running Mach wave (characteristic) is moving toward the right at the speed of sound relative to the fluid element. Hence, the right-running characteristics is propagating to the right (relative to the nozzle) at a combined velocity of $V_1 + a_1$.What we see here is that the right-running characteristic is propagating from point 1 into the domain of the calculation.

The method of characteristics tells us that at a boundary where one characteristic propagates into the domain, then the value of one dependent flow-field variable must be specified at that boundary, and if one characteristic line propagates out of the domain, then the value of another dependent flow-field variable must be allowed to float at the boundary, i.e., it must be calculated in steps of time as a function of the timewise solution of the flow field. Also, note that at point 1 a streamline flows into the domain, across the inflow boundary. In terms of denoting what should and should not be specified at the boundary, the streamline direction plays the same role as the characteristic directions; i.e., the streamline moving into the domain at point 1 stipulates that the value of a second flow-field variable must be specified at

the inflow boundary. Conclusion: At the subsonic inflow boundary, we must stipulate the values of two dependent flow-field variables, whereas the value of one other variable must be allowed to float.

Let us apply the above ideas to the outflow boundary, located at grid N in Fig. 5. As before, the left-running characteristic at point N propagates to the left at the speed of sound, a, relative to a fluid element. However, because the speed of the fluid element itself is supersonic, the left-running characteristic is carried down-stream at the speed (relative to the nozzle) of $V_N - a_N$. The right-running characteristic at point N propagates to the right at the speed of sound *a* relative to the fluid-element, and thus it is swept downstream at the speed (relative to the nozzle) of $V_N + a_N$. Hence, at the supersonic outflow boundary, we have both characteristics propagating out of the domain; so does the streamline at point N. Therefore, there are no flow-field variables which require their values to be stipulated at the supersonic outflow boundary; all variables must be allowed to float at this boundary.

The above discussion details how the inflow and outflow boundary conditions are to be handled on an analytical basis. The numerical implementation of this discussion is carried out as follows.

Subsonic inflow boundary (point 1).

Here, we must allow one variable to float; we choose the velocity V_1, because on a physical basis we know the mass flow through the nozzle must be allowed to adjust to the proper steady state, and allowing V_1 to float makes the most sense as part of this adjustment. The value of V_1 changes with time and is calculated from information provided by the flow-field solution over the internal points. (The internal points are those not on a boundary,i.e., points 2 through N-1 in Fig.3). We use linear exploitation from points 2 and 3 to calculate V_1. This is illustrated in Fig. 6.

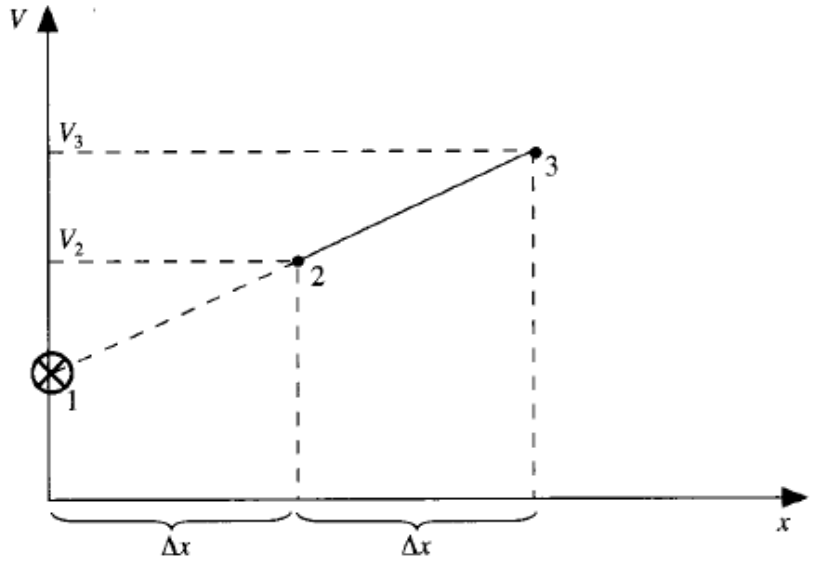

Fig.6. Sketch for linear extrapolation

Here, the slope of the linear extrapolation line is determined from points 2 and 3 as

$$\text{slope} = \frac{V_3 - V_2}{\Delta x}$$

Use this slope to find V_1 by linear extrapolation, we have

$$V_1 = V_2 - \frac{V_3 - V_2}{\Delta x}\Delta x$$

$$\text{or,} \quad V_1 = 2V_2 - V_3 \tag{62}$$

All other flow-field variables are specified. Since point 1 is viewed as essentially the reservoir, we stipulate the density and temperature at point 1 to be their respective stagnation values, ρ_0 and T_0, respectively. They are held fixed, independent of time. Hence, in terms of the nondimensional variables, we have

$$\left.\begin{aligned}\rho_1 &= 1\\ T_1 &= 1\end{aligned}\right\} \text{fixed, independent of time} \tag{63}$$

Pseudocode:

```
% Boundary condition @ first node
    V(1) = 2*V(2)-V(3);
    rho(1) = 1;
    T(1) = 1;
    P(1) = 1;
    M(1) = V(1)*T(1)^-0.5;
```

Supersonic outflow boundary (point N) :

Here, we must follow all flow-field variables to float. We again choose to use linear extrapolation based on the flow-field values at the internal points. Specifically, we have, for the nondimensional variables,

$$V_N = 2V_{N-1} - V_{N-2} \tag{64a}$$

$$\rho_N = 2\rho_{N-1} - \rho_{N-2} \tag{64b}$$

$$T_N = 2T_{N-1} - T_{N-2} \tag{64c}$$

Pseudocode:

```
% Boundary condition @ last node
    V(end) = 2*V(end-1)-V(end-2);
    rho(end) = 2*rho(end-1)-rho(end-2);
    T(end) = 2*T(end-1)-T(end-2);
    P(end) = rho(end)*T(end);
```

```
M(end) = V(end)*T(end)^-0.5;
```

NOZZLE SHAPE AND INITIAL CONDITIONS: The nozzle shape, A = A(x), is specified and held fixed, independent of time. For the case illustrated in this section, we choose a parabola area distribution given by

$$A = 1 + 2.2(x - 1.5)^2 \qquad 0 \le x \le 3 \tag{65}$$

Pseudocode :

```
% Parabolic area distrubition along the nozzle
 A = 1+2.2.*(x-1.5).^2;                          % Area,A/A*
```

Note that x = 1.5 is the throat of the nozzle, that the convergent section occurs for x < 1.5, and that the divergent section occurs for x > 1.5. The nozzle shape is drawn to scale in Fig. 7.

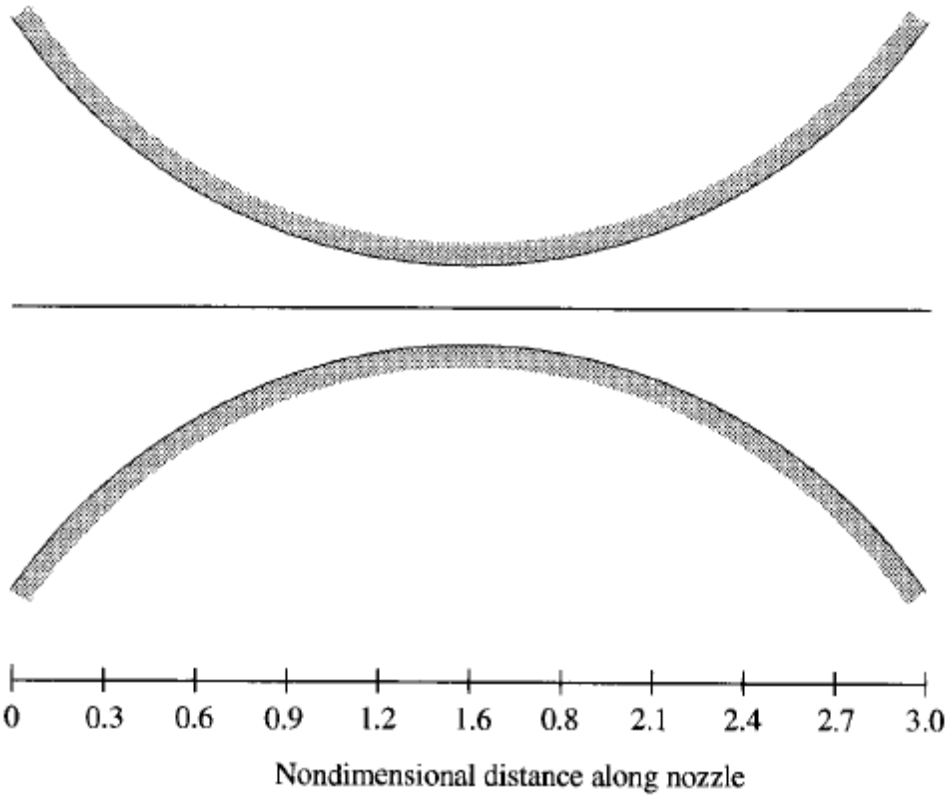

Fig.7. Shape of the nozzle used for the present calculations

Pseudocode for grid point distribution along the nozzle :

```
dx = 0.1;                                    % grid size

% Discretization of nondimensional distance along the nozzle
x = 0:dx:3.0;
```

```
k = length(x);
n = 25;
```

In this problem, we have assumed flow properties across cross-section to be same. So, we discretize the 2D nozzle as follows.

Pseudocode:

```
% Grid distribution in the nozzle

 for i = 1:k
    y = linspace(-A(i)/2,A(i)/2,n);
    for j = 1:n
        xx(i,j) = x(i);
        yy(i,j) = y(j);
    end
end
```

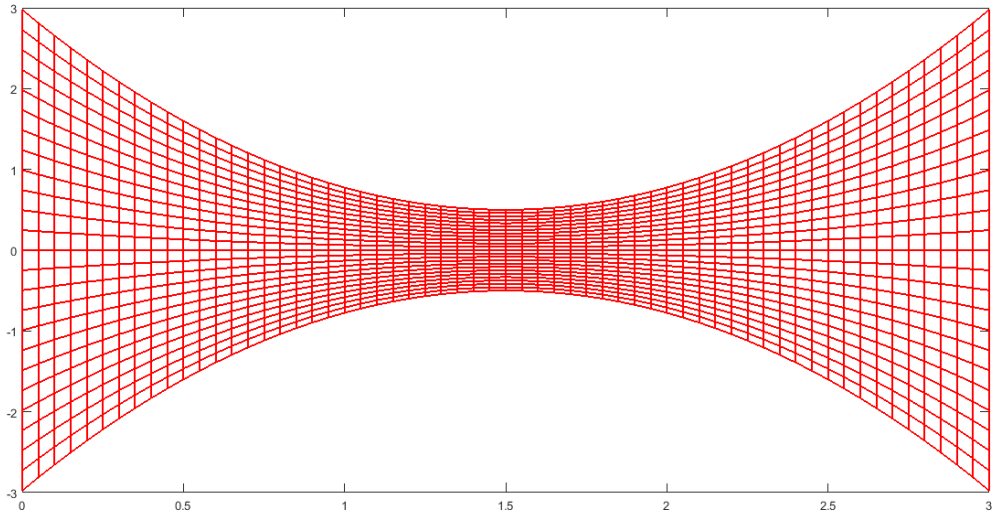

To start the time-marching calculations, we must stipulate initial conditions for ρ, T, and V as a function of x; that is ,we must set up values of ρ, T, and V at time t = 0. In theory, these initial conditions can be purely arbitrary. In practice there are two reasons why you need to choose initial conditions intelligently.

1. The closer the initial conditions are to the final steady-state answer, the faster the time-marching procedure will converge, and hence the shorter will be the computer execution time.
2. If the initial conditions are too far away from reality, the initial timewise gradients at early time steps can become huge; i.e., the time derivatives themselves are initially very large. For a given time step Δt and a given spatial resolution Δx , the large gradients during the early part of the time-stepping procedure can cause the program to go unstable. At the beginning of the calculation, it is wise not to pick initial conditions which can create solution unstable.

We assume the following values at time t = 0

$$\left.\begin{aligned}\rho &= 1-0.3146x \\ T &= 1-0.2314x \\ V &= (0.1+1.09x)T^{1/2}\end{aligned}\right\}\text{initial conditions at } t=0 \qquad \begin{aligned}&(66a)\\&(66b)\\&(66c)\end{aligned}$$

Pseudocode:

```
% Initial Condition
rho = 1-0.3146.*x;            % density,rho/rho0
T = 1-0.2314.*x;              % Temperature,T/T0
V = (0.1+1.09.*x).*T.^0.5;    % Velocity,V/a0
P = rho.*T;                   % Pressure, P/P0
M = V.*T.^-0.5;               % Mach number,M = V/a0/a/a0
mf = rho.*A.*V;               % mass flow rate
```

The full code is given below :

```
clc
close all
clear all

%%%%%-----------------------------------------------
%%%%%
%%%%%-----------------------------------------------
%%%%%

% This program deals with the quasi-one-dimensional
% subsonic-supersonic isentropic
% flow through a convergent-divergent nozzle
% The finite difference expression is set up using
% MacCormack's explicit technique for the numerical
solution
% of governing equations given by Eqs (46),(48) & (50)


%%%%%-----------------------------------------------
%%%%%
%%%%%-----------------------------------------------
%%%%%
```

```
% Note : All parameters are nondimensionalized.


dx = 0.1;                                       % grid size
c  = 0.5;                                       % courant
number
gamma = 1.4;                                    % Ratio of
specific heats

% Discretization of nondimensional distance along the
nozzle
x = 0:dx:3.0;
k = length(x);
n = 25;

% Parabolic area distrubition along the nozzle
A = 1+2.2.*(x-1.5).^2;                                  %
Area,A/A*


% Grid distribution in the nozzle

for i = 1:k
    y = linspace(-A(i)/2,A(i)/2,n);
    for j = 1:n
        xx(i,j) = x(i);
        yy(i,j) = y(j);
    end
end

figure(1)
plot(xx,yy,'-r',xx',yy','-r')

% % Initialization

drhodt_av = zeros(1,k);
dVdt_av = zeros(1,k);
dTdt_av = zeros(1,k);
dta = zeros(1,k);

% Initial Condition
```

```
rho = 1-0.3146.*x;                          %
density,rho/rho0
T = 1-0.2314.*x;                            %
Temperature,T/T0
V = (0.1+1.09.*x).*T.^0.5;                  % Velocity,V/a0
P = rho.*T;                                 % Pressure,
P/P0
M = V.*T.^-0.5;                             % Mach number,M
= V/a0/a/a0
mf = rho.*A.*V;                             % mass flow
rate

mf_0 = mf;                                  % mass flow
rate @ t = 0
gamma1 = 1/gamma;
gamma2 = gamma-1;

resmax = 10^-8;
res = 1;
t = 0;
nstep = 0;

while res > resmax
    prev1 = drhodt_av;
    prev2 = dVdt_av;
    prev3 = dTdt_av;

    for i = 1:k
        dta(i) = (c*dx)/(T(i)^0.5+V(i));
    end
    dt = min(dta);

    % Predictor Step
    for i = 2:k-1;
        V1 = (V(i+1)-V(i))/dx;
        lnA1 = (log(A(i+1))-log(A(i)))/dx;
        rho1 = (rho(i+1)-rho(i))/dx;
        T1 = (T(i+1)-T(i))/dx;
        drhodt_1(i) = -rho(i)*V1-rho(i)*V(i)*lnA1-
V(i)*rho1;                    % eq. (43)
```

```
        dVdt_1(i) = -V(i)*V1-gamma1*T1-
gamma1*rho1*T(i)/rho(i);                % eq. (44)
        dTdt_1(i) = -V(i)*T1-gamma2*T(i)*V1-
gamma2*T(i)*V(i)*lnA1;                  % eq. (45)
    end

    % predicted values
    for i = 2:k-1
        rho_p(i) = rho(i)+drhodt_1(i)*dt;
% eq. (46)
        V_p(i) = V(i)+dVdt_1(i)*dt;
% eq. (47)
        T_p(i) = T(i)+dTdt_1(i)*dt;
% eq. (48)
    end

    t = t+dt;
    nstep = nstep +1;

    rho_p(1) = rho(1);
    V_p(1) = V(1);
    T_p(1) = T(1);

    % corrector step
    for i = 2:k-1;
        V1 = (V_p(i)-V_p(i-1))/dx;
        lnA1 = (log(A(i))-log(A(i-1)))/dx;
        rho1 = (rho_p(i)-rho_p(i-1))/dx;
        T1 = (T_p(i)-T_p(i-1))/dx;
        drhodt_2(i) = -rho_p(i)*V1-
rho_p(i)*V_p(i)*lnA1-V_p(i)*rho1;       % eq. (49)
        dVdt_2(i) = -V_p(i)*V1-gamma1*T1-
gamma1*rho1*T_p(i)/rho_p(i);            % eq. (50)
        dTdt_2(i) = -V_p(i)*T1-gamma2*T_p(i)*V1-
gamma2*T_p(i)*V_p(i)*lnA1;  % eq. (51)
    end

    % Average time derivatives

    for i = 2:k-1;
```

```
        drhodt_av(i) = 0.5*(drhodt_1(i)+drhodt_2(i));
% eq. (52)
        dVdt_av(i) = 0.5*(dVdt_1(i)+dVdt_2(i));
% eq. (53)
        dTdt_av(i) = 0.5*(dTdt_1(i)+dTdt_2(i));
% eq. (54)
    end

    % corrected values of flow field variables at time
t+dt

    for i = 2:k-1
        rho(i) = rho(i)+drhodt_av(i)*dt;
% eq. (55)
        V(i) = V(i)+dVdt_av(i)*dt;
% eq. (56)
        T(i) = T(i)+dTdt_av(i)*dt;
% eq. (57)
        P(i) = rho(i)*T(i);
        M(i) = V(i)*T(i)^-0.5;
    end

    % Boundary condition @ first node
    V(1) = 2*V(2)-V(3);
    rho(1) = 1;
    T(1) = 1;
    P(1) = 1;
    M(1) = V(1)*T(1)^-0.5;

    % Boundary condition @ last node
    V(end) = 2*V(end-1)-V(end-2);
    rho(end) = 2*rho(end-1)-rho(end-2);
    T(end) = 2*T(end-1)-T(end-2);
    P(end) = rho(end)*T(end);
    M(end) = V(end)*T(end)^-0.5;

    % mass flow rate after t+dt
    mf = rho.*A.*V;

    if nstep == 50
        mf_50 = mf;
```

```
    elseif nstep == 100
        mf_100 = mf;

    elseif nstep == 150
        mf_150 = mf;
    elseif nstep == 200
        mf_200 = mf;
    elseif nstep == 700
        mf_700 = mf;
    end

    res1 = abs(drhodt_av(16));
    res2 = abs(dVdt_av(16));

    if res1 > res2
        res = res1;
    else
        res = res2;
    end

    rho_16(nstep) = rho(16);
    T_16(nstep) = T(16);
    P_16(nstep) = P(16);
    M_16(nstep) = M(16);

end

for i = 1:k
    for j = 1:n
        rho1(i,j) = rho(i);
        T1(i,j) = T(i);
        P1(i,j) = P(i);
        M1(i,j) = M(i);
        V1(i,j) = V(i);
    end
end

figure (2)
    plot(1:nstep,rho_16(1:nstep),'-r','LineWidth',2);
    xlabel('Number of time steps','Fontsize',12)
```

```
    h =
ylabel('$\frac{\rho}{\rho_{0}}$','Interpreter','latex')
;
    h.FontSize=20;
    set(h,'position',get(h,'position')+[-50 0 0]);
    set(h,'rotation',0);

    figure (3)
    plot(1:nstep,T_16(1:nstep),'-k','LineWidth',2);
    xlabel('Number of time steps','Fontsize',12)
    h =
ylabel('$\frac{T}{T_{0}}$','Interpreter','latex');
    h.FontSize=20;
    set(h,'position',get(h,'position')+[-50 0 0]);
    set(h,'rotation',0)


    figure (4)
    plot(1:nstep,P_16(1:nstep),'-b','LineWidth',2);
    xlabel('Number of time steps','Fontsize',12)
    h =
ylabel('$\frac{p}{p_{0}}$','Interpreter','latex');
    h.FontSize=20;
    set(h,'position',get(h,'position')+[-50 0 0]);
    set(h,'rotation',0);

    figure (5)
    plot(1:nstep,M_16(1:nstep),'-g','LineWidth',2);
        xlabel('Number of time steps','Fontsize',12)
    h = ylabel('$M$','Interpreter','latex');
    h.FontSize=20;
    set(h,'position',get(h,'position')+[-50 0 0]);
    set(h,'rotation',0);


% creating file and writing steady state values on it

fid = fopen( 'flow field variables', 'wt' );
fprintf(fid,'x/L     A/A*   rho/rho0   V/a0   T/T0
p/p0     M   mass flow\n')

%fprintf(fid,'%s'/t,'');
```

```
for j = 1:k

    B = [x(j);A(j);rho(j);V(j);T(j);P(j);M(j);mf(j)];
    fprintf(fid,'%.3f %7.3f %7.3f %7.3f %7.3f %7.3f
%7.3f %7.3f\n',B);

end

figure(6)
plot(x,rho,'-k','LineWidth',2)
hold on
plot(x,P,'-g','LineWidth',2)
hold on
plot(x,T,'-b','LineWidth',2)
legend('\rho/\rho_{0}','p/p_{0}','T/T_{0}')
xlabel('Nondimensional distance through nozzle
(x)','FontSize',12)
ylabel('Density ratio,Pressure ratio,Temperature
ratio')

figure(7)
plot(x,mf_0,'--
r',x,mf_50,'r',x,mf_100,'r',x,mf_150,'r',x,mf_200,'r',x
,mf_700,'r')
xt = [2.4 2.4 2.4 2.4 2.4 2.4 ];
i = find(x==2.4);
yt = [mf_0(i)+0.08 mf_50(i)+0.08 mf_100(i)+0.08
mf_150(i)+0.08 mf_200(i)+0.08 mf_700(i)+0.08];
str =
{'0\Deltat','50\Deltat','100\Deltat','150\Deltat','200\
Deltat','700\Deltat'};
text(xt,yt,str)
grid on
xlabel('Nondimensional distance through nozzle
(x)','Fontsize',12)
h = ylabel('Nondimensional mass flow
(\rhoVA)/(\rho_{0}a_{0}A^{*})');
h.FontSize=12;

figure(8)
surf(xx,yy,P1);view(2)
```

```
shading interp
colormap(jet(256))
colorbar
title('Presure distrubtion across the nozzle')
```

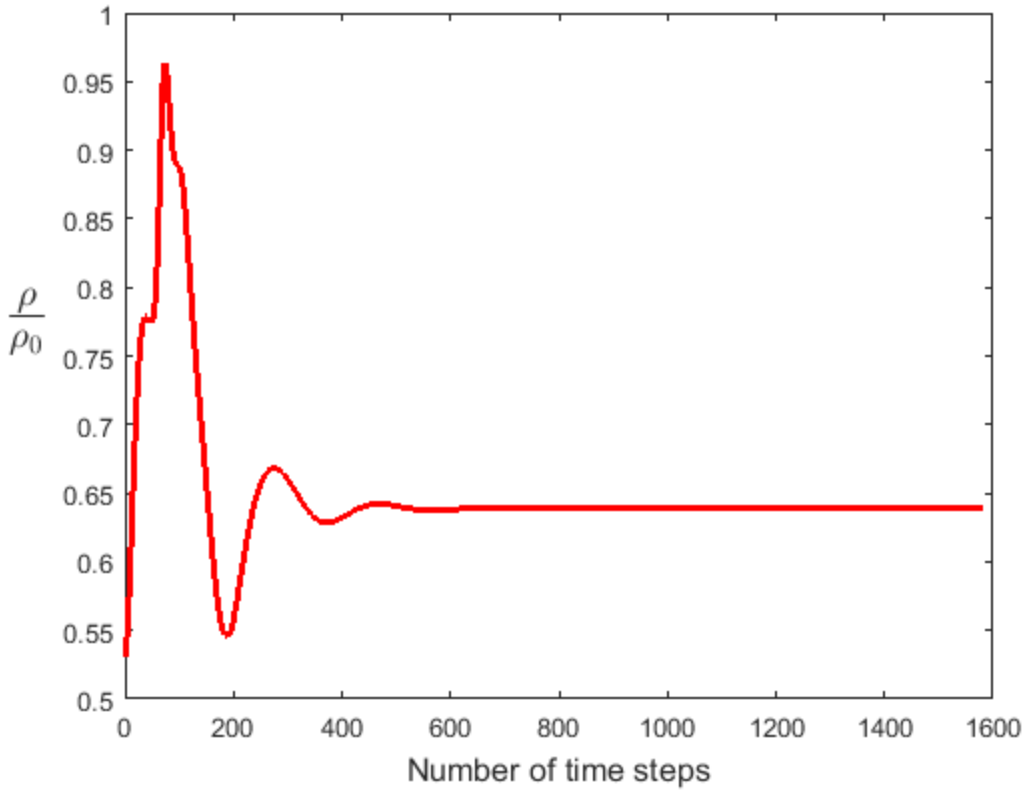

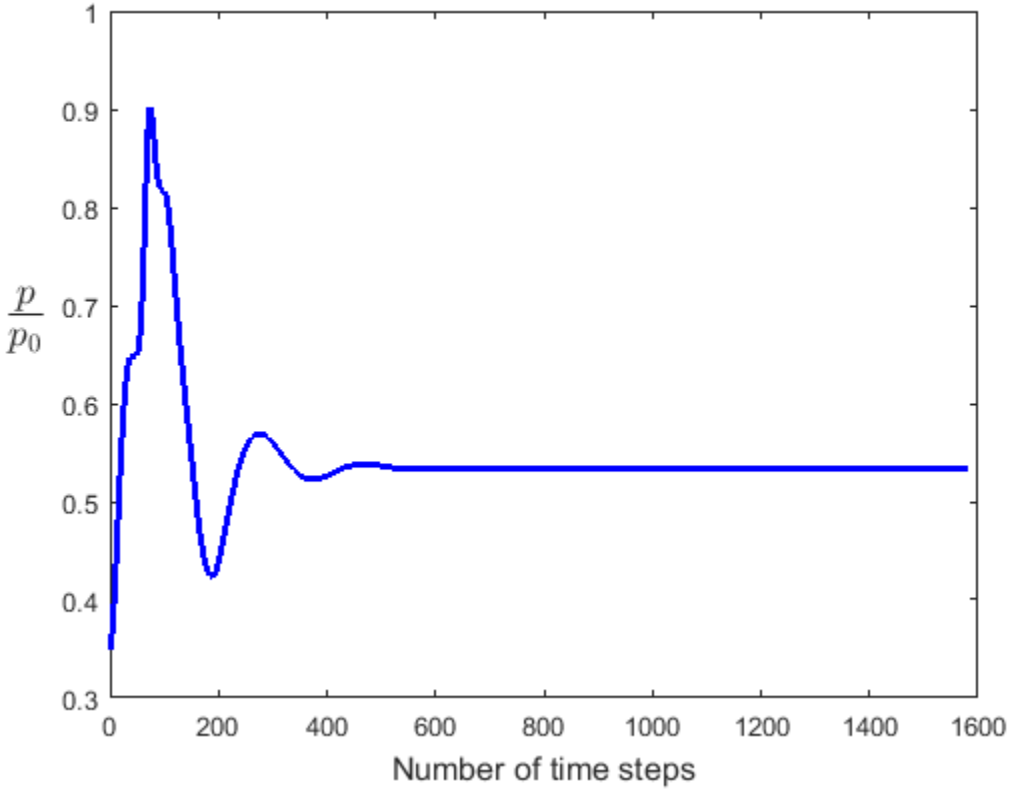
1
0.9
0.8
$\frac{p}{p_0}$
0.7
0.6
0.5
0.4
0.3
0
200
400
600
800
1000
1200
1400
1600
Number of time steps

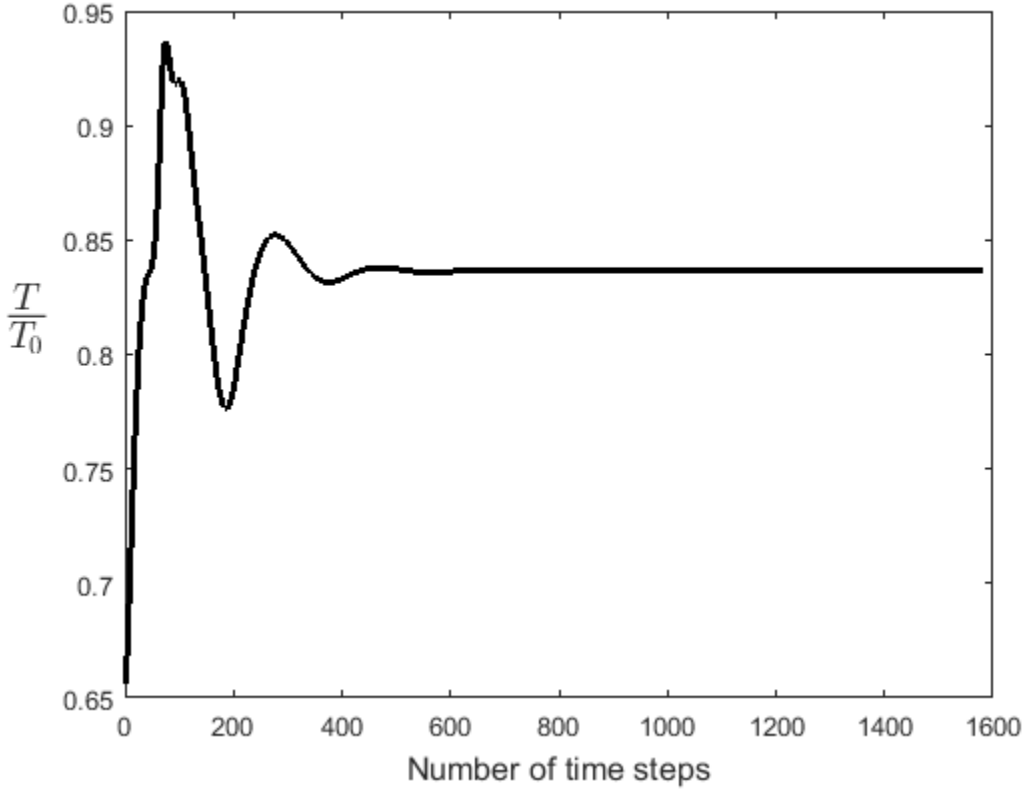
0.95
0.9
0.85
0.8
0.75
0.7
0.65
$\frac{T}{T_0}$
0
200
400
600
800
1000
1200
1400
1600
Number of time steps

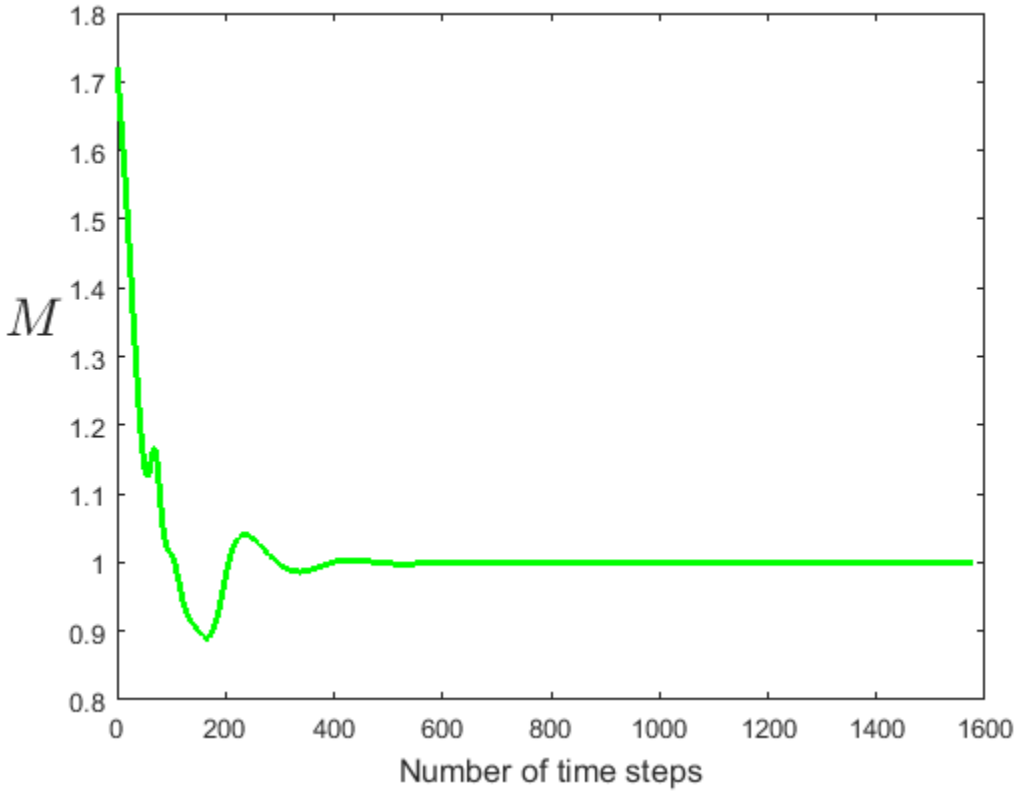
1.8
1.7
1.6
1.5
1.4
1.3
1.2
1.1
1
0.9
0.8
M
0
200
400
600
800
1000
1200
1400
1600
Number of time steps

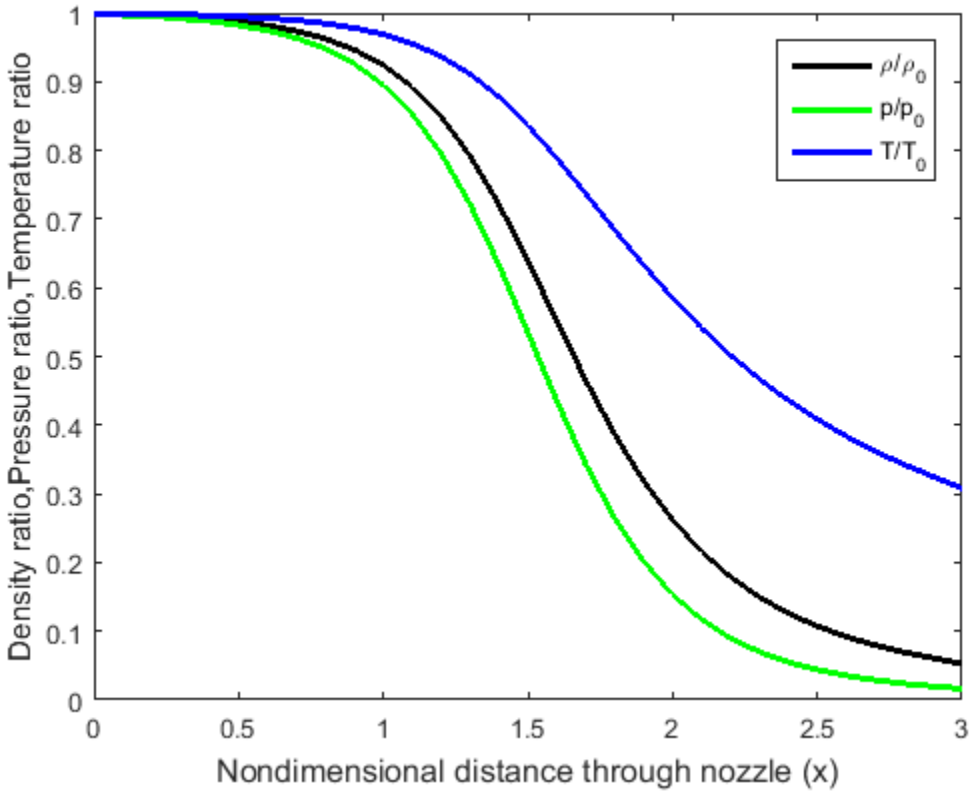
Density ratio,Pressure ratio,Temperature ratio
Nondimensional distance through nozzle (x)
ρ/ρ0
p/p0
T/T0
0
0.1
0.2
0.3
0.4
0.5
0.6
0.7
0.8
0.9
1
0
0.5
1
1.5
2
2.5
3

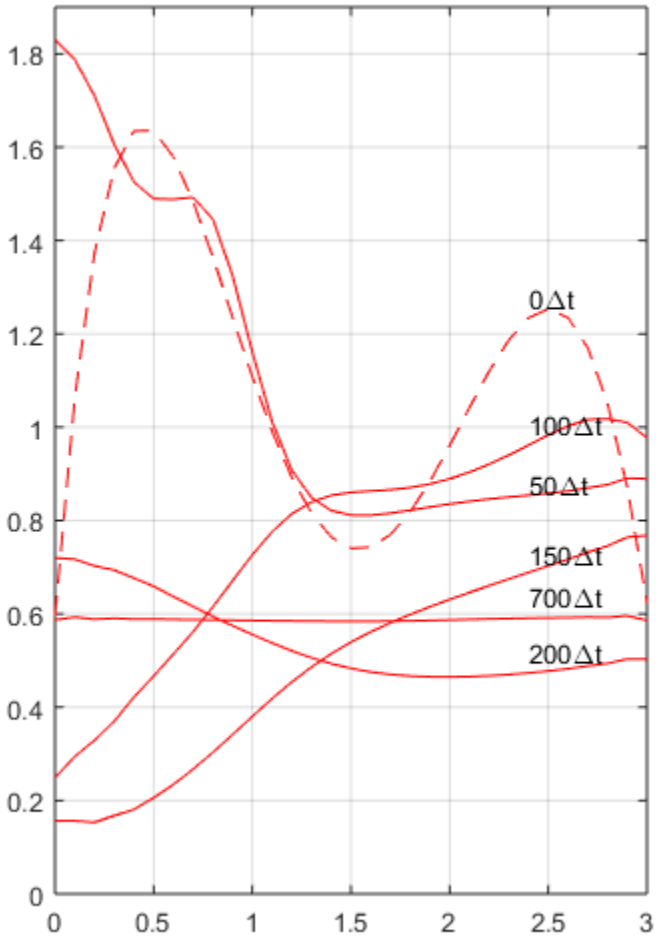
1.8
1.6
1.4
1.2
1
0.8
0.6
0.4
0.2
0
0
0.5
1
1.5
2
2.5
3
0Δt
100Δt
50Δt
150Δt
700Δt
200Δt

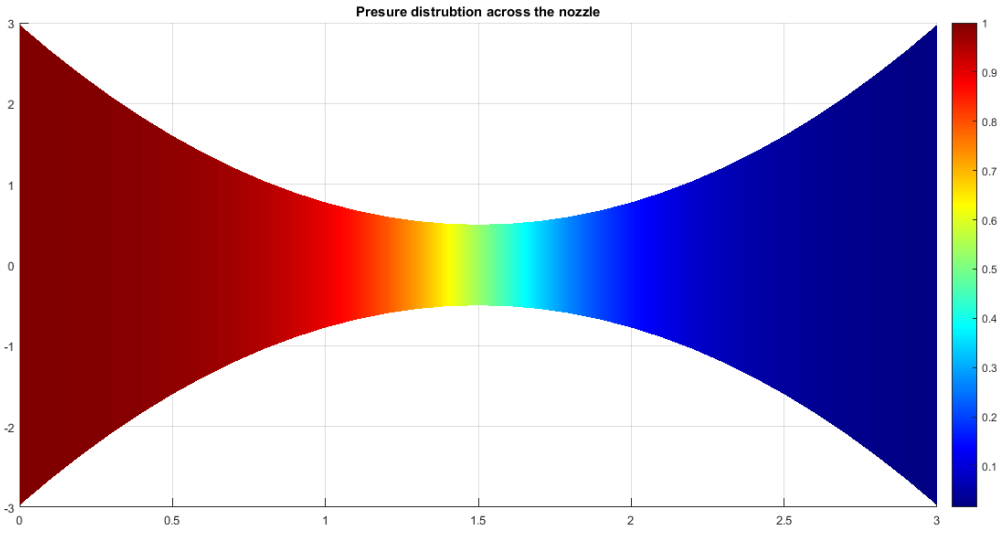
Presure distrubtion across the nozzle
3
2
1
0
-1
-2
-3
0
0.5
1
1.5
2
2.5
3
1
0.9
0.8
0.7
0.6
0.5
0.4
0.3
0.2
0.1